

# High-strength economically alloyed corrosion-resistant steels with the structure of nitrogen martensite

**O Bannykh, V Blinov and E Lukin**

Institute of Metallurgy and Material Science RAS, Leninskiy av. 49, Moscow, 119991, Russia

**Email:** bannykh@imet.ac.ru

**Abstract.** The use of nitrogen as the main alloying element allowing one both to increase the corrosion resistance and mechanical properties of steels and to improve their processability is a new trend in physical metallurgy of high-strength corrosion resistant steels. The principles of alloying, which are developed for high-nitrogen steel in IMET RAS, ensure the formation of the structure, which contains predetermined amounts of martensite (70-80%) and austenite (20-30%) and is free from  $\delta$ -ferrite,  $\sigma$ -phase, and  $\text{Cr}_{23}\text{C}_6$  carbide. These principles were used as the base for the creation of new high-strength corrosion-resistant weldable and deformable 0Kh16AN5B, 06Kh16AN4FD, 08Kh14AN4MDB, 09Kh16AN3MF, 27Kh15AN3MD2, 40Kh13AN3M2, and 19Kh14AMB steels, which are operative at temperatures ranging from -70 to 400°C. The developed nitrogen-containing steels compared with similar carbon steels are characterized by a higher resistance to pitting and crevice corrosion and are resistant to stress corrosion cracking. The new steels successfully passed trial tests as heavy duty articles.

## 1. Introduction

New and very wide possibilities of the application in different industrial branches are opened for corrosion-resistant steel with the structure of nitrogen martensite. The urgency of such steels, which can reliably operate under the joint actions of high static, cyclic, and dynamic loads as well as cavitation and corrosion-active media, is determined by the fact that the reserves of improvement in the level and combination of the above properties of conventional stainless steels are almost exhausted. The most widely used stainless steel with the structure of nitrogen martensite is the 1Kh15N5AM3 steel (the Russian VNS-5 grade and the international AM-350 and AM-355 grades) [1, 2]. However this carbon containing steel in large sections tends to the precipitation of grain-boundary chromium carbides, which abruptly decreases the crack resistance at low temperatures ( $\text{CRT} = 5 \text{ J/cm}^2$ ) and the resistance to stress corrosion cracking in salt spray chambers ( $\sigma_{\text{cc}} = 300 \text{ MPa}$ ). Furthermore, this steel contains expensive molybdenum.

## 2. Results

As a result of studying the effects of alloying elements as well as heat treatment and thermomechanical treatment regimes on the structure, physicomechanical, chemical, and technological properties, our Institute developed new high-strength corrosion-resistant weldable and deformable 0Kh16AN5B, 06Kh16AN4FD, 08Kh14AN4MDB, 09Kh16AN3MF, 27Kh15AN3MD2, 40Kh13AN3M2 and 19Kh14AMB steels with the structure of nitrogen martensite (Table 1) [3, 4].



**Table 1.** Mechanical properties of the new high-strength corrosion-resistant Cr-Ni-N steels.

Steel	Treatment*	Mechanical properties			
		$\sigma_B$ (MPa)	$\sigma_{0.2}$ (MPa)	$\delta$ (%)	$\Psi$ (%)
05Kh16AN5B(0.13% N)	H.R. + Q. 1000°C + T. 400°C	1530	1320	23	68
	C.R. $\varepsilon = 25\%$	1850	1760	10	46
08Kh14AN4MDB(0.19% N)	H.R. + Q. 1050°C + T. 500°C	1664	1466	19	61
	Q. 1050°C + C.R. $\varepsilon = 25\%$	1920	1877	14	53
09Kh13AMB (0.21% N)	H.R. + Q. 950°C – air	1928	1625	7	16
19Kh14AMB (0.15% N)	H.R. + Q. 950°C – air	1949	1548	8.5	30
40Kh13AN3M2 (0.13% N)	F + C.T.-196°C + T. 200°C	2083	1454	12	10
09Kh16AN3MF (0.19% N)	H.R. + Q. 1090°C + C.T. -70°C + +T. 450°C	1780	1546	16	49
	H.R. + Q. 1090°C + T. 200°C + +T. 400°C	1785	1500	17	59
	H.R. + C.T. -196°C + T. 400°C	1880	1740	12	43

\*H.R. – hot rolling, F. – forging, C.R. – cold rolling, Q. – quenching, T. – tempering, C.T. – cold treatment

The Kh15N5-type steel additionally alloyed with nitrogen, molybdenum, and copper and microalloyed with vanadium and rare-earth metals [3] was selected as the basis for the development of high-strength economically alloyed stainless steel.

Formation of the martensitic-austenitic structure providing a combination of high strength, corrosion resistance, and workability is achieved under the following conditions:

$$\begin{aligned}
 12 < Cr_{eqv} < 17; & & 9 < Ni_{eqv} < 14; \\
 Cr = 12.0 \div 17.0; & & C = 0.05 \div 0.25; \\
 Mo = 0 \div 2.0; & & N = 0.10 \div 0.25; \\
 V = 0 \div 0.1; & & Ni = 0 \div 5.0; \\
 Nb = 0 \div 0.1; & & Cu = 0 \div 2.0; \\
 & & 0.15 < C + N < 0.50;
 \end{aligned}$$

Such correlations of alloying elements in the steel provide the martensitic-austenitic structure ( $M = 70 \div 80\%$ ,  $A = 20 \div 30\%$ ) and the absence of  $\delta$ -ferrite,  $\sigma$ -phase, and  $Me_{23}C_6$  type carbides in the structure, while the thermoplastic processing provides a grain size of 5 - 15 microns. The formation of such structures provides improved corrosion resistance, strength, ductility, and workability in the conditions of manufacturing articles of complex shapes and various sizes.

The indicated carbon and nitrogen concentrations in the steel are necessary for the attainment of high strength. As the carbon and nitrogen contents exceed 0.30 and 0.20%, respectively, it is difficult to reach satisfactory levels of plasticity and impact toughness and to obtain a high-quality metal free from porosity caused by a limited solubility of nitrogen in steel.

The aim of the 12.0-17.0% Cr addition is to provide the desired corrosion resistance and to increase nitrogen solubility. As the chromium and nickel concentrations exceed 17.0% and 2.5%, respectively, the steel is low-ductile, especially at low temperatures, because of the appearance of  $\delta$ -ferrite, which elevates the ductile-brittle transition temperature. As the nickel content exceeds 5%, the nitrogen solubility in the steel decreases.

The aim of the addition of 0.5-1.5% manganese is to increase the nitrogen solubility and, of course, the steel deoxidation. As the manganese concentration exceeds 1.5%, the content of retained austenite increases, and this deteriorates the strength characteristics of the steel.

The addition of 0.1% vanadium provides the formation of fine-grained structure. At higher vanadium contents, the strength of the steel decreases because the solid solution becomes depleted of nitrogen because of the formation of vanadium nitrides.

Alloying with 0.5-2.0% molybdenum improves the corrosion resistance, increases the solubility of nitrogen, and inhibits the formation of carbonitrides at grain boundaries and thereby improves the impact toughness of the steel.

Alloying with 1.0-2.0% copper allows one to eliminate the delta ferrite in the microstructure and to improve the corrosion resistance and strength as a result of aging with the precipitation of fine particles of the copper-rich phase.

The presence of 0.005-0.030% cerium and 0.005-0.030% calcium helps to reduce the content of impurities at grain boundaries, thereby altering the kinetics of particle formation at the boundaries and reducing the degree of embrittlement. Alloying with lanthanum and yttrium promotes deoxidation and grain refinement of the steel.

According to the Scheffler diagram, the chromium equivalent ( $Cr_{eqv}$ ) should range from 12 to 17, and the nickel equivalent ( $Ni_{eqv}$ ) should range from 9 to 14. This correlation provides the absence of  $\delta$ -ferrite,  $\sigma$ -phase, and  $Cr_{23}C_6$  chromium carbides in the structure (Figure 1).

The solubility limit of nitrogen in the steel was calculated using the interaction parameters obtained by Feichtinger [4]. The calculation showed that the solubility of nitrogen in such steels at maximum content of elements raising and lowering the solubility varies from 0.20 to 0.12%, respectively.

Mechanical and technological properties of such steels substantially depend on their phase composition.

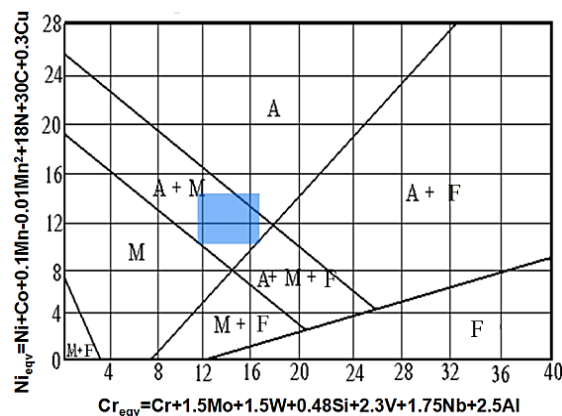


**Figure 1.** A. Scheffler phase diagram of corrosion-resistant steels.

The change in the phase composition and lattice parameters of the  $\alpha$ - and  $\gamma$ -phases directly upon heating from 20 to 1000°C is shown (Figure 2) by the example of the 08Kh14AN4MDB steel [6]. At room temperature, the contents of  $\alpha$ - and  $\gamma$ -phases are 78 and 22%, respectively. Upon heating to a temperature of 600°C, the phase composition remains virtually unchanged. However, starting from 300°C, the temperature dependence of the  $\alpha$ -phase lattice parameter (Figure 2a) deviates from a straight line, and this shows that the nitrogen concentration in this phase reduces because of the precipitation of fine chromium nitride particles.

The temperature dependence of the  $\gamma$ -phase lattice parameter (Figure 2b) shows positive deviation from a straight line, especially at temperatures above 400°C. This shows that the nitrogen content in austenite increases. The  $\alpha \rightarrow \gamma$  transformation begins at temperatures above 600°C (Figure 2a), and the austenite content reaches 50% at 700°C and then increases to 80% at 800°C and to 100% at 1000°C.

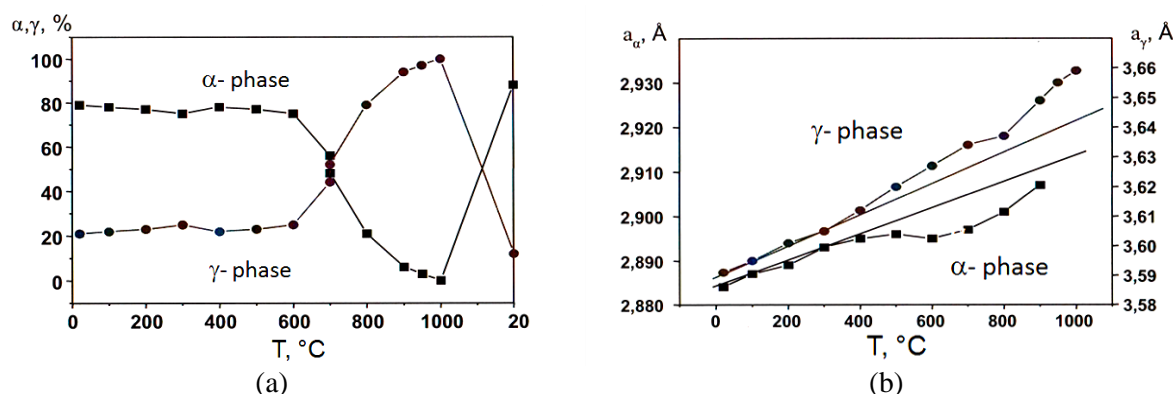


**Figure 2.** Changes in the phase composition and lattice parameters of the 08Kh14AN4MDB steel upon heating in a range of 20 - 1000°C [6].

In a temperature range of 600-800°C, the temperature dependence of the  $\gamma$ -phase lattice parameter (Figure 2b) is parallel to the line corresponding to the effect of linear expansion, and this indicates that the nitrogen content in the  $\gamma$ -phase is constant. Above 800°C, the slope of the temperature dependence of the lattice parameter substantially grows, suggesting that the nitrogen content in austenite in these temperature conditions increases.

The above results [6] can be interpreted as follows. The initial sample quenched from 1050°C contains  $\alpha$ -phase (~80%), austenite, and fine particles of chromium nitride precipitated from austenite upon its decomposition in the process of quenching. Upon heating, the  $\alpha$  phase at 300-600°C decomposes with the precipitation of nitride and, possibly, carbide phases. Thus, the nitrogen content decreases in martensite and increases in austenite. At 600-800°C, the  $\alpha$  phase transforms to austenite, and this is accompanied by dissociation of nitrides. At temperatures of 800-1000°C, the transformation of the  $\alpha$ -phase to austenite is completed, and the nitrogen content in it continuously increases. The dissolution of the nitride phase in austenite in this temperature range is intensified and is completed at 1000°C, as is evidenced by a sharp increase in austenite grain size [6].

The hardness, grain size, and amounts of the  $\alpha$  and  $\gamma$  phases of the steels depend on heat treatment conditions (Figure 3). As the temperature of heating for water quenching increases from 950 to 1150°C, the hardness of the 08Kh14AN4MDB steel is reduced from 43 to 36 HRC, and the grain size is increased from 15 to 110 microns (Figure 3a) [6, 7]. According to the XRD data (Figure 3b), the decrease in the steel hardness with increasing quenching temperature is caused by the reduction in martensite content and the increase in the content of retained austenite.

The characteristic structure of the steels after quenching consists of packet martensite with interlayers of retained austenite (Figures 4a and 4b) [7].

According to the established [7] specific features of the quenched 08Kh14AN4MDB steel structure, the retained austenite is present in several morphological versions: in the form of thin layers at the boundaries of  $\alpha$ -crystals inside the packets (Figures 4c and 4d), in the form of sufficiently broad, extended regions between  $\alpha$ -crystals in the packets and at the junctions of packets (Figure 4), and in the form of sufficiently long randomly shaped regions near the boundaries of former austenite grains (Figure 4d).

The high level of the steel strength is reached after tempering as a result of the precipitation of fine carbonitride particles [7-10]. A maximum strength level of 497-507 HV for the 08Kh14AN4MDB steel quenched from 1050 - 1100 °C is achieved after tempering at 500°C for 0.5-2 hours. This can be attributed to the formation of fine carbonitride particles upon tempering. Tempering at 600 and 700°C leads to the carbonitride coagulation resulting in softening of the steels.

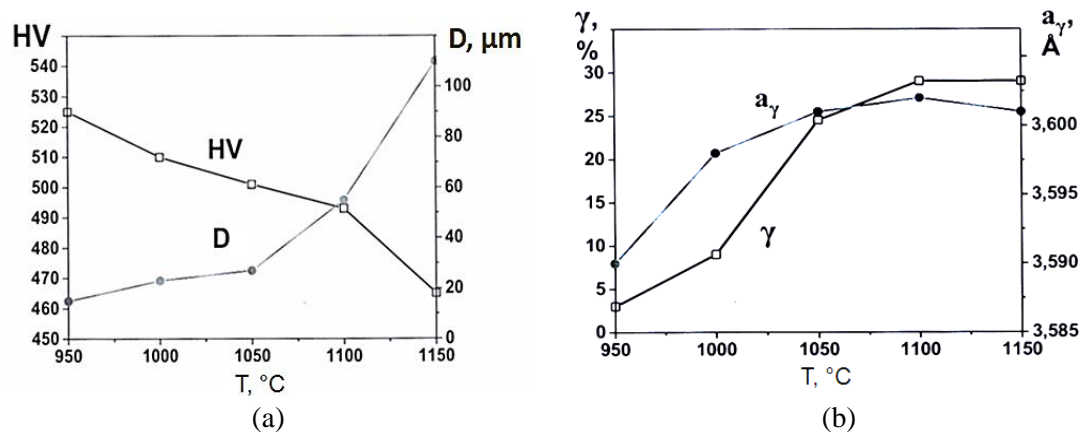


**Figure 3.** Effect of quenching temperature on the structure (a) and properties (b) of the 08Kh14AN4MDB steel [7].

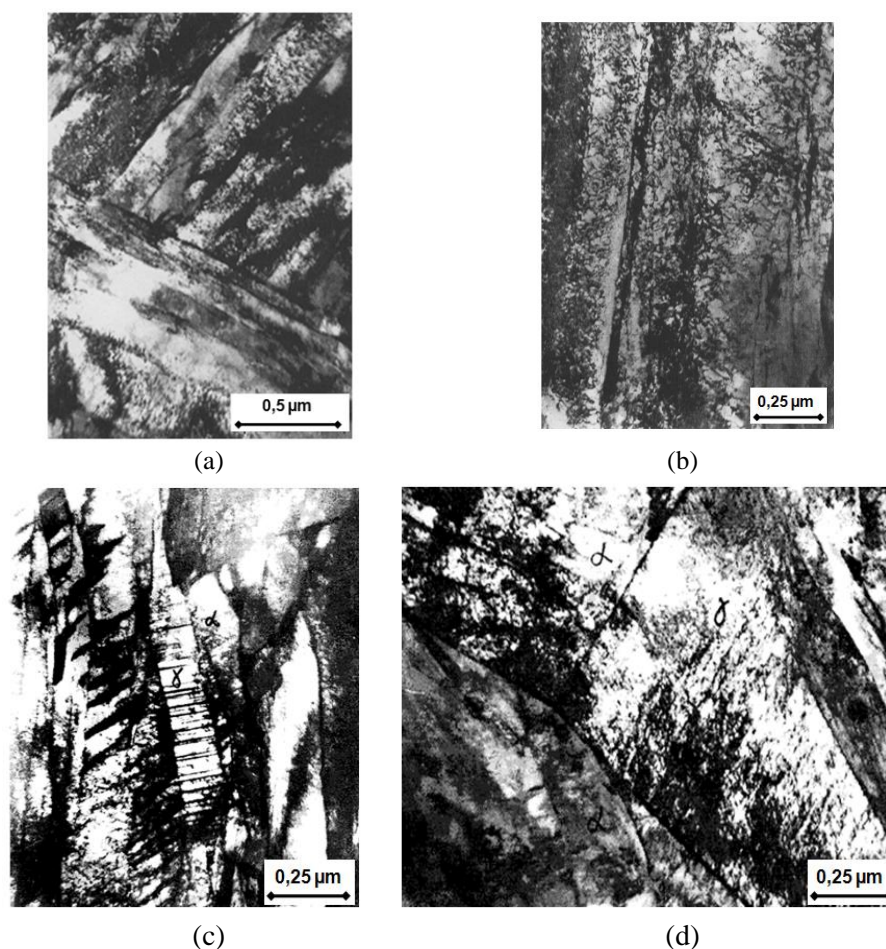


**Figure 4.** Microstructure of the 08Kh14AN4MDB steel after quenching from 1050°C [7].

Fine precipitates (Figures 5a and 5b) were observed after tempering in the structure of the 08Kh14AN4MDB steel. The coarsest precipitates reach 70 nm in length and 15 nm in width. Their

density is relatively low, and they are distributed relatively uniformly within the  $\alpha$ -crystals. The particles are also precipitated at the  $\alpha$ -crystal boundaries [7].

The tensile tests of the steels at elevated temperatures showed that the 05Kh16AN5 steel after quenching from 1000°C and tempering at 400°C and the 08Kh14AN4MDB steel after quenching from 1050°C, cold treatment at -70°C, and tempering at 500°C are insignificantly softened at temperatures up to 500°C (Table 2).

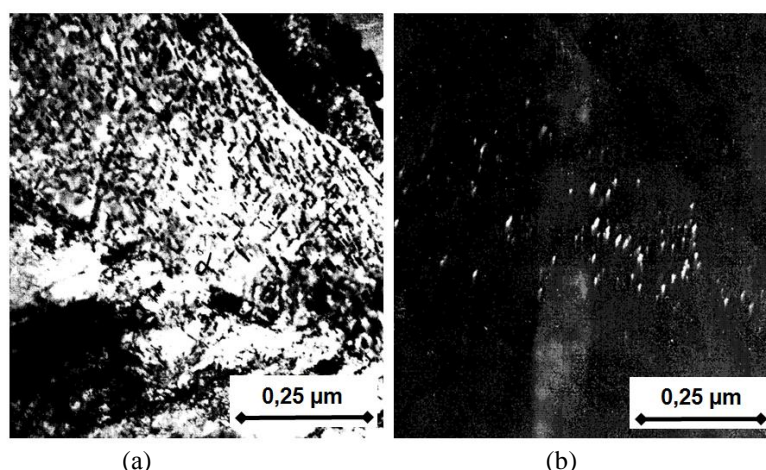


**Figure 5.** Microstructure of the 08Kh14AN4MDB steel after quenching from 1050°C and tempering at 500°C: (a) bright-field image and (b) dark-field image [7].

**Table 2.** Mechanical properties at different test temperatures of the 05Kh16AN5B steel (after quenching from 1000°C and tempering at 400°C) and the 08Kh14AN4MDB steel (after quenching from 1050°C, cold treatment at -70°C, and tempering at 500°C) [7].

Steel	Test temperature (°C)	$\sigma_B$ (MPa)	$\sigma_{0,2}$ (MPa)	$\delta$ (%)	$\Psi$ (%)
05Kh16AN5B	20	1450	1125	23	68
	300	1170	1000	19	49
	400	1090	932	15	49
	500	980	821	10	56
	600	570	527	7	75
08Kh14AN4MDB	20	1595	1070	14	45
	300	1200	1035	10	42
	400	1170	990	9	42
	500	1000	885	7	45
	600	660	604	4	62

Thermomechanical treatment of the 14Kh15AN4M steel is accompanied by drastic changes not only in the phase composition, but also in the substructure of individual phases [11, 12]. Deformation leads to the austenite decomposition, and the resulting martensite inherits the austenitic-matrix deformation defects, which are added by the lattice defects caused by martensitic transformation upon cooling of the steel after rolling. The latter is related also to the austenite, which adds the transformation-induced strengthening upon the martensitic transformation to the substructure formed by rolling. These effects can be quantitatively estimated from the  $\alpha$ - and  $\gamma$ -phase diffraction reflection widths (Figures 6 and 7), which are proportional to the accumulated deformation energy or the density of lattice defects.

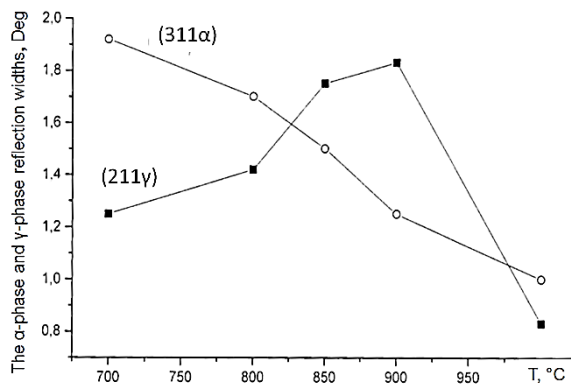


**Figure 6.** Widths of the (211)  $\alpha$ -phase and (311)  $\gamma$ -phase reflections as a function of rolling temperature for the 14Kh15AN4M steel (a reduction of 70%) [11].

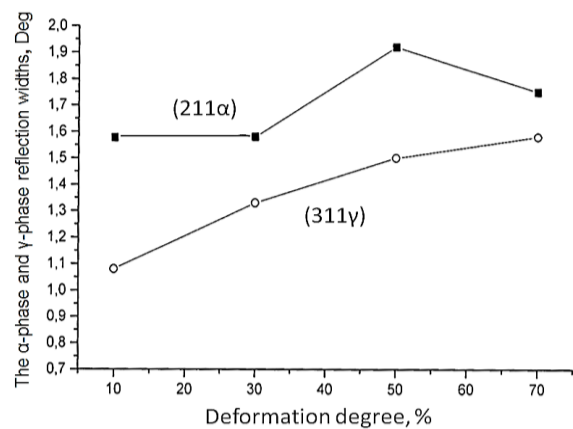


**Figure 7.** Widths of the (211)  $\alpha$ -phase and (311)  $\gamma$ -phase reflections as a function of the degree of deformation after rolling of the 14Kh15AN4M steel at a temperature of 850°C [11].

Change the  $\alpha$ -phase reflection width in Figure 6 is nonmonotonic. An increase in the defect density in the martensite crystal lattice with increasing rolling temperature from 700 to 900°C virtually coincides with the change in the austenite content, i.e., in fact, the defect density of martensite lattice is inversely proportional to the martensite content. This can be explained only by the fact that, unlike austenite, in which lattice defects are mainly caused by deformation and are uniformly distributed throughout the volume, martensite is characterized by the maximum defect density localized at the martensite/austenite interface. An abrupt reduction in the density of crystal defects at a temperature of 1000°C (Figure 6) is due, first, to decrease in the density of defects inherited from the matrix and, second, to decrease in fraction of the martensite/austenite interfaces relative to that observed after rolling at 900°C (Figure 6).

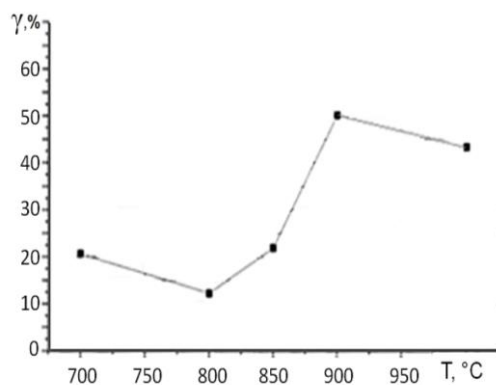


**Figure 8.** Effect of rolling temperature (reduction of 70%) on the austenite content in the 14Kh15AN4M steel [11].

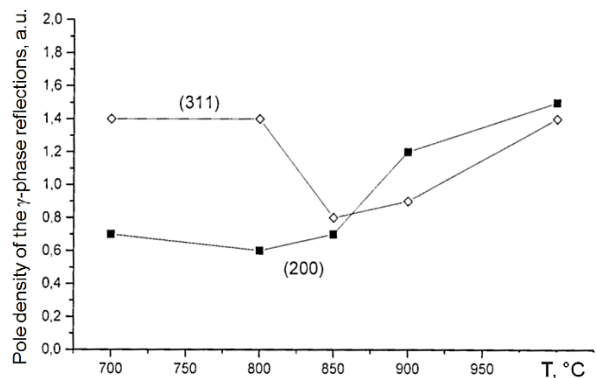


**Figure 9.** Pole density of the (200) and (311)  $\gamma$ -phase reflections as a function of rolling temperature (reduction of 70%) for the 14Kh15AN4M steel [11].

The monotonic increase in the defect density in the austenite with increasing degree of deformation at 850°C (Figure 7) is quite natural and is associated with increasing work hardening of the phase, in which deformation occurs. The defect density in martensite in much lesser extent varies with increasing degree of deformation. In this case, the effect of the degree of deformation on the reflection

width is opposite to its effect on the austenite content (Figure 8), while the analogous dependences on temperature (Figures 6 and 8) are similar in character. This result requires a further study because it shows important features of the steel behavior upon thermomechanical processing.

Figures 9 and 10 show the dependences of the pole densities of various  $\gamma$ -phase reflections on rolling temperature and on the degree of deformation, respectively. They can be used to estimate the texture formation as a function of rolling conditions. We can conclude that no pronounced texture is formed under all deformation conditions, even in the austenite, which is directly subjected to deformation. This suggests the occurrence of dynamic recrystallization of austenite upon rolling, which is accompanied by the nucleation and growth of grains free from any preferred orientation. The martensite formed from the textureless matrix moreover should not have any preferred orientation, since the occurring multivariate transformation results in a textureless martensite state even in the case of a pronounced matrix texture [11].

A higher strength level of the steels is achieved by cold rolling. An increase in the total reduction to 75% upon cold rolling of the 08Kh14AN4MDB steel increases the martensite content from 79 to 96% (Figure 11), and this enhances the hardness from 40 to 55 HRC (Table 3). The accompanying growth of martensite tetragonality in the 08Kh14AN4MDB steel from 1.0033 to 1.0124 can be attributed to more substantial imperfection of its crystal lattice (Table 4). As the degree of reduction ranges between 10 and 25%, deformation of austenite occurs preferably without any martensite formation, and this leads to high strengthening at insignificant decrease in ductility (Figure 11). Warm rolling of the steels at 300, 400, 500 and 600°C with an increase in the total degree of reduction to 75% also results in increased hardness to 50-53, 51-52, 49-53, and 43-44 HRC, respectively (Table 3).

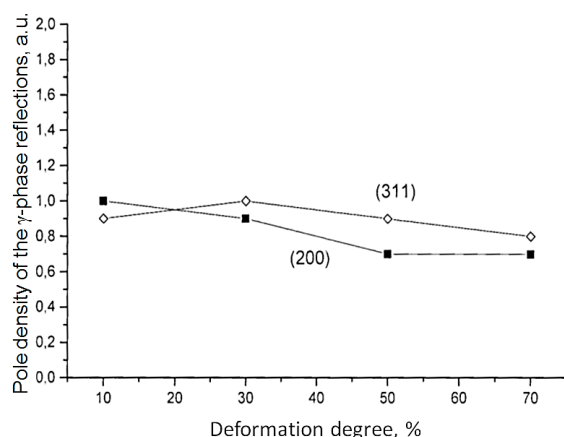


**Figure 10.** Pole density of the (200) and (311)  $\gamma$ -phase reflections of the 14Kh15AN4M steel as a function of the degree of deformation at 850°C [11].

**Table 3.** Hardness of the 08Kh14AN4MDB steel after quenching from 1050°C and rolling at various temperatures to various degrees of reduction [12].

Degree of reduction, %	Rolling temperature (°C)				
	20	300	400	500	600
0	40	41	41	42	38
25	48	44	44	44	40
30	50	46	46	47	41
45	52	49	49	51	42
60	55	50	50	52	43
75	55	53	52	53	44

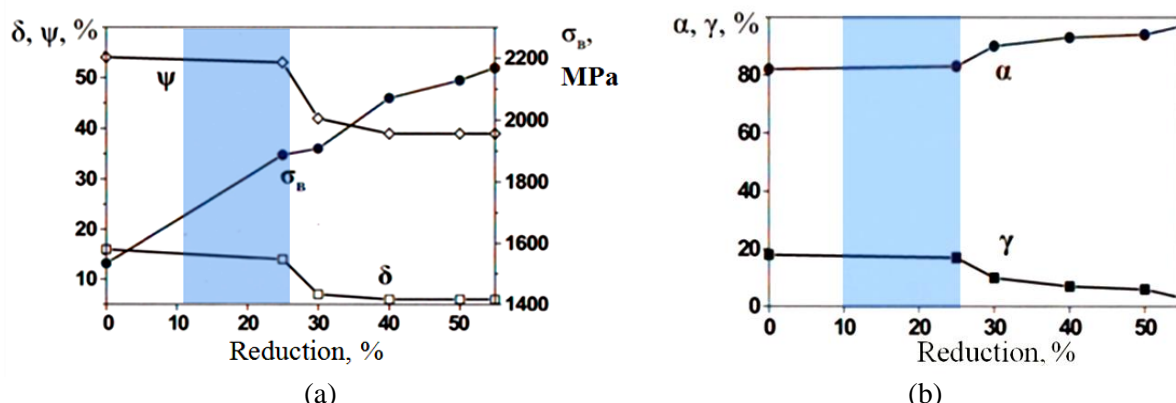


**Figure 11.** Mechanical properties (a) and the  $\alpha$ - and  $\gamma$ -phase contents (b) of the 08Kh14N4AMBD steel after quenching from 1050°C and subsequent cold rolling to different reductions [12]. The highlighted areas correspond to the optimum degrees of reduction upon rolling.

At a small degree of reduction (25%) upon cold rolling, the steels undergo mainly deformation of austenite without formation of martensite. This leads to high strengthening of austenite with a slight decrease in ductility (Figure 3). Rolling to a reduction of 30-55% leads to a higher strengthening due to the deformation of martensite formed upon quenching and the formation of stress-induced martensite from austenite ( $\gamma \rightarrow \alpha$  transformation). However, this is accompanied by a significant decrease in ductility of the steel. According to the X-ray diffraction data, an increase in the degree of reduction above 25% upon cold rolling increases the content and tetragonality (imperfection) of martensite (Table 4).

**Table 4.** Austenite lattice parameter and martensite tetragonality of the 08Kh14AN4MDB steel after quenching from 1050°C and cold rolling to various degrees of reduction [12].

Degree of reduction (%)	Austenite lattice parameter and martensite tetragonality	
	$a_\gamma$ (Å)	c/a
0	3.601	1.0033
25	3.592	1.0034
30	3.592	1.0066
45	3.598	1.0071
50	3.596	1.0096
60	3.596	1.0109
65	3.594	1.0118
75	3.593	1.0124

The 05Kh16AN5 steel after quenching from 1000°C and tempering at 400°C for 2 h and the 08Kh14AN4MD steel after quenching from 1050°C and tempering at 500°C for 2 h have high fatigue strength (Figure 12) [9]. A higher fatigue limit based on loading  $10^7$  cycles is characteristic of the 05Kh16AN5 steel.

Corrosion resistance of the 05Kh16AN5B and 08Kh14AN4MDB steels can be considered as a function of the contents of chromium and nitrogen as well as heat treatment conditions [13]. The optimum heat treatment regimes for the experiments evaluating corrosion resistance are as follows: quenching from 1000-1050°C and tempering at 400 - 600°C.

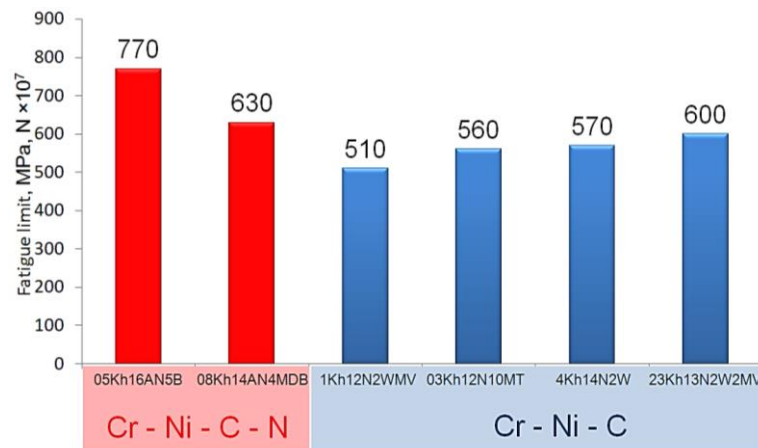


**Figure 12.** Fatigue strength of commonly used corrosion-resistant Cr-Ni-Cu martensitic steels and new Cr-Ni-N-C martensitic-austenitic steels [9].

The results of the study of general corrosion demonstrated that the corrosion rate of the martensitic-austenitic nitrogen-containing 05Kh16AN5 and 08Kh14AN4MDB steels as well as the austenitic 08Kh18N10T steel after all heat treatment conditions decreases with increasing duration of holding in 3.5% NaCl solution. A typical dependence of such attenuation of corrosion with increasing duration of the contact with a corrosive medium is shown in Figure 13 [13].

In the conditions under consideration, the worst corrosion resistance is exhibited by the 08Kh18N10T austenitic steel. The quenched steel in corrosion resistance ranks significantly below the 05Kh16AN5 08Kh14AN4MDB steels. However, the precipitation of carbonitride particles slightly increases corrosion rate of the latter steels.

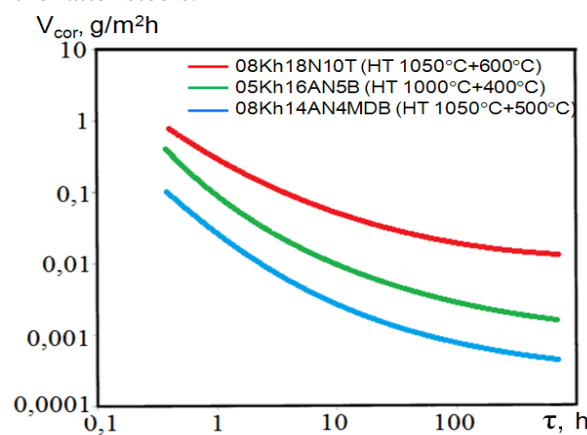


**Figure 13.** Corrosion resistance of the 08Kh14AN4MDB, 0Kh16AN5B, and 08Kh18N10T steels in 3.5% NaCl solution [13].

The results on the corrosion kinetics of the 08Kh14AN4MDB steel after tempering at 400 and 500°C (Figure 13) show that, regardless of the tempering temperature, the corrosion rate decreases by a factor of more than 25 as the holding time in the corrosive medium increases from 20 to 530 hours. The study of this steel revealed that the ratio between the martensite and austenite contents and the degree of their decomposition in tempered steel insignificantly affect their corrosion resistance in the NaCl solution.

Upon short-term holdings (20 hours), the 08Kh14AN4MDB steel exhibits a tendency to decreasing corrosion rate with elevating tempering temperature. Longer holdings lead to the growth of corrosion rate with elevating tempering temperature [12].

### 3. Summary

The technical effects of the creation of the new corrosion-resistant low-carbon steels with the structure of nitrogen martensite are as follows:

- the development of a new class of corrosion-resistant structural steels exceeding analogous steels in strength will provide a breakthrough in the field the design of advanced machines, instruments and constructions and improving the existing ones;
- an improvement in the reliability and service life of such products at a simultaneous reduction in the cost of their manufacture as a result of using cost-effective materials and processes, which do not require the development of new metallurgical equipment.

### Conclusions

1. The chemical composition, which upon quenching and tempering of the steel provides the structure with predetermined contents of martensite (70-80%) and austenite (20-30%) and is free from  $\delta$ -ferrite,  $\sigma$ -phase, and  $\text{Cr}_{23}\text{C}_6$  type chromium carbides, has been selected and justified for the realization of improved characteristics of strength, ductility, and corrosion resistance of economically alloyed chromium-nickel-nitrogen steels.
2. The phase transformations occurring upon heating and cooling of chromium-nickel-nitrogen steels free from molybdenum and copper (05Kh16AN5B) and containing these elements (08Kh14AN4MDB) have been studied. The temperature dependences of the  $\alpha$ - and  $\gamma$ -phase contents, the  $\alpha \rightarrow \gamma$  transformation temperature range (600-800°C), and the temperatures (300°C) of the start of the precipitation and complete dissociation (1050°C) of chromium carbonitrides in the 08Kh14AN4MDB steel are determined. In the 05Kh16AN5 steel, the  $\alpha \rightarrow \gamma$  transformation begins and ends at temperatures of 470 and 680°C, respectively.
3. The optimum quenching temperatures providing almost complete chromium carbonitride dissolution at the retention of fine-grained structure (with an average grain size of about 27-29  $\mu\text{m}$ ) have been established to be 1000°C for the 05Kh16AN5 steel and 1050°C for the 08Kh14AN4MDB steel.
4. The specific features of the structure of retained austenite, which is present in the quenched 08Kh14AN4MDB steel both in the form of thin layers between martensite crystals and in the form of massive regions with a high density of dislocations and twins, have been revealed by electron microscopy.
5. It is shown that the structure of packet martensite with thin interlayers of retained austenite free from fine precipitates is retained in the 08Kh14AN4MDB steel after quenching from 1050°C and tempering at 400°C. The strengthening fine carbonitride particles up to 70 nm long and 15 nm thick are present in the steel structure after quenching from 1050°C and tempering at 500°C.
6. The maximum strengthening of the 05Kh16AN5 steel ( $\sigma_{\text{B}}=1833$  MPa) and the 08Kh14AN4MDB steel ( $\sigma_{\text{B}}=2168$  MPa) is achieved by cold rolling to a reduction of 50-55%. These steels have the best combinations of mechanical properties after cold rolling to a reduction of 25% (the 05Kh16AN5 steel:  $\sigma_{\text{B}}=1680$  MPa,  $\sigma_{0.2}=1410$  MPa,  $\delta=18\%$ ,  $\psi=60\%$ ; the 08Kh14AN4MDB steel:  $\sigma_{\text{B}}=1887$  MPa,  $\sigma_{0.2}=1677$  MPa,  $\delta=14\%$ ,  $\psi=53\%$ ) and after warm rolling at temperatures of 300-500°C to a reduction of 60% ( $\sigma_{\text{B}}=1730-1790$  MPa,  $\sigma_{0.2}=1300-1400$  MPa,  $\delta=18-23\%$ ,  $\psi=50-63\%$ ).

### References

- [1] Bratuhin A G 1996 *Technological maintenance of high quality, reliability, service life of aviation equipment* (Moscow: Mashinostroenie) pp 524 (in Russian)
- [2] Voznesenskaya N M, Izotov V I, Ulianova N V, Popova L S and Potak Ya M 1971 *Metal Science and Heat Treatment* **1** 32 (in Russian)

- [3] Kostina M V, Bannykh O A and Blinov V M 2000 *Metal Science and Heat Treatment* **12** 3 (in Russian)
- [4] Satir-Kolorz A H and Feichtinger H 1991 *Mettalkunde* **82** (9) 689
- [5] Kostina M V, Bannykh O A, Blinov V M and Stepanov G A 2002 *Proc. Conf. on Strength mater. and structures at low temp. (Russia, Saint-Petersburg)* 26
- [6] Bannykh O A, Betsofen S Ya, Blinov V M, Il'in A A, Kostina M V and Blinov E V 2006 *Metally* **5** 1 (in Russian)
- [7] Bannykh O A, Blinov V M, Kostina M V, Afanasiev N A, Betsofen S Ya and Adyev S V 2004 *Metally* **6** 3(in Russian)
- [8] Bannykh O A, Blinov V M, Kostina M V Lukin E I, Blinov E V and Rigina L G 2015 *Metally* **4** 72 (in Russian)
- [9] Blinov V M, Bannykh O A, Kostina M V, Nemirovskiy Yu R and Khadyev M S 2000 *Metally* **3** 64
- [10] Bannykh O A, Blinov V M, Shalkevich A B and Voznesenskaya N M 2005 *Metally* **3** 51
- [11] Bannykh O A, Betsofen S Ya, Lukin E I, Blinov V M, Voznesenskaya N M, Tonysheva O A and Blinov E V 2015 *Metally* **1** 32
- [12] Kostina M V, Bannykh O A and Blinov V M 2001 *Metal Science and Heat Treatment* **7** 3
- [13] Blinov V M, Kalinin G Yu, Kostina M V, Mushnokova S Yu, Popova V I and Kharkov A A 2003 *Metally* **4** 84